diversity

MDPI

Article

A Proposed Method for Assessing the Spatio-Temporal Distribution of *Carcharhinus melanopterus* (Quoy and Gaimard, 1824) in Shallow Waters Using a UAV: A Study Conducted in Koh Tao, Thailand

Andrea Di Tommaso, Sureerat Sailar, Francesco Luigi Leonetti, Emilio Sperone * and Gianni Giglio *

Laboratory of Marine Zoology and Herpetology, Department of Biology, Ecology and Earth Sciences, University of Calabria, 87036 Rende, Italy; francescoluigi.leonetti@unical.it (F.L.L.)
* Correspondence: emilio.sperone@unical.it (E.S.); gianni.giglio@unical.it (G.G.); Tel.: +39-0984492972 (E.S.)

Abstract: In this study, we propose a method for assessing the temporal and spatial distribution of *Carcharhinus melanopterus* in shallow waters using unmanned aerial vehicles (UAVs). Aerial surveys were conducted in Tien Og Bay (Koh Tao, Thailand) thrice daily (morning, afternoon, evening) along a 360 m transect at a 30 m altitude. Environmental factors, including cloudiness, sea conditions, wind, tide, and anthropogenic disturbance, were recorded for each time slot. We developed a Python/AppleScript application to facilitate individual counting, correlating sightings with GPS data and measuring pixel-based length. Abundance varied significantly across time slots ($p < 0.001$), with a strong morning preference, and was influenced by tide ($p = 0.040$), favoring low tide. Additionally, abundance related to anthropogenic disturbance ($p = 0.048$), being higher when anthropogenic activity was absent. Spatial distribution analysis indicated time-related, sector-based abundance differences ($p < 0.001$). Pixel-based length was converted to Total Length, identifying juveniles. They exhibited a strong sector preference ($p < 0.001$) irrespective of the time of day. Juvenile abundance remained relatively stable throughout the day, constituting 94.1% of afternoon observations. Between 2020 and 2022, an underwater video survey was conducted to determine the sex ratio of the individuals. Only females and juveniles were sighted in the bay.

Keywords: unmanned aerial vehicles; sharks; ecology

check for updates

Citation: Di Tommaso, A.; Sailar, S.; Leonetti, F.L.; Sperone, E.; Giglio, G. A Proposed Method for Assessing the Spatio-Temporal Distribution of *Carcharhinus melanopterus* (Quoy and Gaimard, 1824) in Shallow Waters Using a UAV: A Study Conducted in Koh Tao, Thailand. *Diversity* **2024**, *16*, 606. https://doi.org/10.3390/d16100606

Received: 28 June 2024
Revised: 15 September 2024
Accepted: 18 September 2024
Published: 1 October 2024

Copyright: © 2024 by the authors. Licensee MDPI, Basel, Switzerland. This article is an open access article distributed under the terms and conditions of the Creative Commons Attribution (CC BY) license (https://creativecommons.org/licenses/by/4.0/).

1. Introduction

Carcharhinus melanopterus (Quoy and Gaimard, 1824) is one of the most abundant sharks inhabiting islands, atolls, and coastal waters from the Red Sea to the Indian Ocean and the central Pacific [1–3].

The high population density observed when direct threats are absent suggests that it exerts a certain influence on coral ecosystems [2,4]. In 2020, it was classified as vulnerable by IUCN mainly because of the shrinkage of the population across the last three generations due to fishing and habitat destruction.

Carcharhinus melanopterus is a medium-sized shark (<1.80 m TL) that reaches maturity between 0.9 and 1.34 m TL [2,5,6]. The reproductive cycle is biennial [2] and is characterized by placental viviparity. Two–four pups measuring 0.3–0.5 m TL [5,7] are delivered after 7 to 16 months' gestation [7,8]. In the Great Barrier Reef, it has been estimated that maturity is reached around 4.2 years for males and 8.5 years for females. Captive specimens can reach a life span of 25 years [6]. The duration of a generation is estimated to be 14.5 years.

Carcharhinus melanopterus inhabits shallow waters even less than one meter in depth, but has been found in water up to a depth of 75 m [5]. In addition to coral reefs, it also colonizes turbid waters and mangroves [7,9]. The coastal habits make it an easy species to observe and consequently a possible tourist attraction, which is also due to

its low aggressiveness towards humans, making up around 3% of the total recorded shark attacks [10]. It feeds mainly on small fish, crustaceans, and mollusks, but also snakes [11], birds, and even rats in specific locations such as Australia, Seychelles, and French Polynesia [10,12].

The species is often observed forming aggregations [13] and has a high site-fidelity [2,12]. This has led some authors to suppose that the patterns with which aggregations occur may be stable over time [13]. The site-fidelity makes *Carcharhinus melanopterus* an ideal model with which to study social structure and aggregation patterns in elasmobranchs, and to determine by which factors they are influenced. Currently, there is no evidence of territoriality in elasmobranchs [14]; however, hierarchies based on size may exist. Some scholars have hypothesized that fin markings of some species may play a role in the species-specific recognition and size assessment of other individuals in sharks such as *Triaenodon obesus* (whitetip reef shark) and *Carcharhinus melanopterus* [15].

This study aims to contribute to the knowledge of the ecology of the Blacktip reef shark, particularly in Tien Og Bay (Thailand). In order to optimize data collection in the natural environment, a method for assessing the temporal and spatial distribution of *Carcharhinus melanopterus* in shallow waters using unmanned aerial vehicles (UAVs) is proposed.

Over the past decade, drones, BRUVS, and other new technologies have become a popular tool for shark research [16,17]. In particular, the rapid proliferation of the drone technology has enabled new studies in the field of shark research, focused mainly on shark hazard reduction [18], shark predation events [19], shark behavior, and social interactions [20,21], but also pelagic shark aggregations [22]. Drone technology has also been successfully used to study the ecology and behavior of reef sharks [23], where field studies often suffer from objective difficulties in collecting data. In fact, shallow reefs are generally only accessible by foot at low tides or by boat at high tides; this makes using common abundance or behavior survey techniques difficult to use effectively.

In these shallow reef environments, drones currently provide one of the only means to study shark behavior, distribution, and abundance. The use of drones in these environments, however, is relatively novel, and there are few studies that have relied on this approach to obtain relevant data. Furthermore, it is also necessary to work on data collection and analysis methodologies to develop protocols that allow for optimizing costs and times and obtaining quality data [24].

Study Area

The research was conducted in Tien Og Bay (Figure 1), located in the southeast of Koh Tao, Thailand. Koh Tao is a 21 km^2 granitic island situated 72 km from the mainland. The waters surrounding the island are home to coral communities that, under the most favorable conditions, can form a fringing reef [25]. Tien Og Bay is commonly referred to as Shark Bay due to the relative ease with which *Carcharhinus melanopterus* can be observed.



Figure 1. Tien Og Bay, located in the southeast of Koh Tao, Thailand.

The bay has an extensive beach of fine coral sand in a North–North-West position, in front of the Haad Tien resort. On both rocky sides, other resorts are found, from which it is possible to access the bay. The seabed, starting from the Haad Tien Resort beach, is initially sandy. After a few meters, it presents the first isolated coral structures which gradually become more aggregated. Living corals alternate with dead coral rubble, which sometimes serve as a substrate for macroalgae. Granite boulders are sparsely distributed and colonized by corals of the genus *Porites* spp., forming structures known as "mini-atolls" due to the characteristic morphology they assume when the low depth of the water limits their growth in height. Proceeding out to sea—in the South–South-East direction—after about 200 m from the beach, the seabed reaches a depth of 2–3 m and a thick layer of dead Acropora rubble can be found, alternately colonized by the macroalgae *Turbinaria* spp., living Acropora, and sponges. The main tourist activity is SCUBA diving. The island has 67 diving schools [26], making it the second largest location in the world for the number of SCUBA certifications issued per year [27]. Diving, snorkeling, and marine traffic exert a significant pressure on the system, sometimes physically damaging shallow-water coral structures [28,29]. In recent years, some Thai beaches have been closed to the public to allow ecosystems to recover from the strong anthropogenic pressure. The case of Maya Bay in Phi Phi Islands is remarkable, which, a few months after its closure to the public in 2018, registered a massive aggregation of *Carcharhinus melanopterus.*

The following shark species have historically been present in Koh Tao coastal waters:

- *Rhincodon typus* (whale shark);
- *Carcharhinus melanopterus* (Blacktip reef shark);
- *Carcharhinus amblyrhynchos* (Gray reef shark);
- *Carcharhinus leucas* (Bull shark);
- *Triakis semifasciata* (Leopard shark).

In recent years, only *Carcharhinus melanopterus* and, exceptionally, the whale shark *Rhincodon typus* have been found [30].

2. Materials and Methods

The study was carried out between 19 August 2021 and 9 September 2021. A DJI Mini 2 drone, DJI Official Store Bangkok (Bangkok, Thailand) was used in manual flight for data collection. The DJI Mini 2 is equipped with a 1/2.3″ 12MP CMOS sensor and a 4.49 mm lens (equivalent to 24 mm in full-frame format), with an 83° viewing angle and a maximum aperture of f/2.8.

For data collection, a transect of about 360 m was covered at an average speed of 2 m/s 4 times (2 round trips) for each time slot 3 times a day (07:00, 13:00, 18:00), except in cases of extremely bad weather conditions. Videos were recorded with a resolution of 2.7 K (2720 × 1530) at 30 fps. In total, we recorded (details in Table 1) the following:

- 07:00—20 videos, from 20 August to 9 September 2021;
- 13:00—16 videos, from 19 August to 4 September 2021;
- 18:00—14 videos, from 19 August to 4 September 2021.

For each time slot, the following environmental factors were recorded. A discrete numerical value was assigned to each condition as follows:

1. Cloudiness—0: clear (0–2 Oktas); 1: partly cloudy (3–5 Oktas); 2: cloudy (6–8 Oktas); 3: rain (after/before).
2. Wind—0: absent (0 m/s wind speed); 1: weak (1–2 m/s wind speed); 2: medium (3–5 m/s wind speed); 3: strong (5–10 m/s wind speed); 4: very strong (>10 m/s wind speed).
3. Tide—0: low; 1: medium; 2: high.
4. Sea condition—0 (0–1 Beaufort scale): flat; 1: quiet (2–3 Beaufort scale); 2: almost quiet (4 Beaufort scale).
5. Anthropogenic disturbance—0: absent; 1: snorkeling/kayaking; 2: motorboat.

Table 1. Activity table for each sampling day. W and R, respectively, represent NA due to wind or rain.

Date	Morning Transect Time	Afternoon Transect Time	Evening Transect Time
19 August 2021		13:10	18:08
19 August 2021	06:54	13:06	18:07
21 August 2021	07:06	13:04	18:02
22 August 2021	07:07	13:00	18:04
23 August 2021	07:06	12:55	17:59
24 August 2021	06:59	13:10	W
25 August 2021	07:15	13:04	18:07
26 August 2021	07:09	13:12	17:42
27 August 2021	07:05	12:53	17:59
28 August 2021	07:11	13:07	18:06
29 August 2021	09:23	13:09	18:03
30 August 2021	06:57	13:09	17:59
31 August 2021	07:08	R	R
01 September 2021	08:50	13:05	17:59
02 September 2021	07:03	13:23	W
03 September 2021	07:03	13:04	18:03
04 September 2021	08:18	13:10	18:04
05 September 2021	07:05		
06 September 2021	07:15		
07 September 2021	R		
08 September 2021	07:10		
09 September 2021	07:09		

Considering the presence of swimmers, boats, and infrastructures, a height of 30 m was chosen in accordance with Thai legislation about drones, which requires a minimum distance of 30 m from people, vehicles, and infrastructures.

The starting point was established in accordance with the distance of at least 30 m from the nearby resorts. The end point was chosen based on the most easily identifiable visual landmark on the other side of the bay: the white building of the Jamahkiri Resort.

Considering the focal length of the drone's lens and the dimensions of the sensor, it has been estimated that, from a height of 30 m, an image corresponding to a width of 41 m on the ground is captured.

The following equation represents the proportional relationship between the length of a line in the real world and the length of a line in pixels on an image:

$$\text{RealWorldLength} = \text{GSD} \times \text{LengthInPixels}$$

The Ground Sampling Distance (GSD), expressed in px/m, indicates how many meters a single pixel in the image corresponds to. The GSD was calculated through the following formula:

$$\text{GSD} = \frac{\text{SensorWidth} \times \text{Altitude}}{\text{FocalLength} \times \text{ImageWidth}} = \frac{6.17\ \text{mm} \times 30\ \text{m}}{4.49\ \text{mm} \times 2720\ \text{px}} = 0.015\ \text{m/px}$$

In our case, we wanted to estimate the entire scene width captured by the sensor; therefore, LengthInPixel = ImageWidth = 2720 px. Given that, the following is obtained:

$$\text{WidthCameraFootprint} = \text{GSD} \times \text{LengthInPixel} = 0.015\ \text{m/px} \times 2720\ \text{px} = 41\ \text{m}$$

2.1. Temporal Data Analysis and Environmental Factors

We flew the transect for two round trips. Each round trip included one leg in the forward direction (labeled A1 and A2, respectively) and one leg in the return direction (labeled R1 and R2), resulting in a total of four legs for the two round trips.

For each video recorded between 20 August 2021 and 04 September 2021, observed individuals were counted for each leg of the transect. The results were grouped by time slot. For each time slot, we created a table reporting the date, actual start time of the video recording, environmental factors (cloudiness, wind, tide, sea conditions, anthropogenic disturbance), and the number of sharks observed in each leg of the transect, labeled nA1, nR1, nA2, and nR2. Table 2 shows the data collected in the morning between 20 August 2021 and 04 September 2021.

Table 2. Data collected in morning time between 20 August 2021 and 04 September 2021: environmental factors and observations for each day. nA1, nR1, nA2, and nR2 represent the observations in each leg of the transect; nMax represents the highest number of observations among the legs of the transect ('abundance'); nTot represents the sum of observations across all the legs of the transect ('activity').

Date	Time	Weather (0–3)	Wind (0–4)	Tide (0–2)	Sea (0–2)	Disturbance (0–2)	nA1	nR1	nA2	nR2	nMax	nTot
20 August 2021	06:54	1	1	0	1	1	20	23	34	32	34	109
21 August 2021	07:06	2	1	0	2	0	13	11	13	14	14	51
22 August 2021	07:07	2	1	0	2	0	7	7	6	10	10	30
23 August 2021	07:06	1	2	0	1	0	22	26	32	31	32	111
24 August 2021	06:59	0	2	0	0	0	8	8	10	16	16	42
25 August 2021	07:15	3	3	1	1	0	3	4	5	4	5	16
26 August 2021	07:09	3	3	1	2	0	4	4	4	6	6	18
27 August 2021	07:05	3	1	1	1	0	6	11	13	18	18	48
28 August 2021	07:11	3	2	1	2	0	5	2	10	6	10	23
29 August 2021	09:23	2	0	0	1	0	28	24	24	16	28	92
30 August 2021	06:57	0	0	1	1	0	0	3	7	4	7	14
31 August 2021	07:08	2	0	0	1	1	4	5	5	4	5	18
01 September 2021	08:50	2	2	0	1	1	3	1	3	3	3	10
02 September 2021	07:03	2	1	0	0	1	12	11	20	8	20	51
03 September 2021	07:03	2	1	0	0	0	9	17	16	13	17	55
04 September 2021	08:18	2	0	0	0	0	NA	NA	NA	NA	NA	NA

We added a column labeled 'nMax', representing the highest number of observations among the legs of the transect, which we considered as abundance. We counted the individuals that entered the screen as soon as they were visible. The linear movement of the UAV at a speed of 2 m/s prevented double counting the same individuals within a leg. A column labeled 'nTot' was added, representing the sum of observations across all the legs of the transect, which we considered the animal's activity. Animal activity is generally defined as the amount of time an animal spends in motion [22]. Most shark species remain in motion throughout their entire lives. When measuring spatial and temporal niche partitioning among a species—such as through camera trapping—ecologists consider every sighting as 'activity' regardless of whether it involves the same or different individuals. Therefore, in our case, nTot may include double-counted individuals, as the drone moving back and forth along a line may encounter the same individuals multiple times. We used this value to compare it with the abundance.

Abundance and activity values, grouped by the 3 time slots, were analyzed to detect statistical significance using the Kruskal–Wallis test.

Abundance and activity values were then aggregated by environmental factors' conditions (cloudiness, wind, tide, sea condition, anthropogenic disturbance), and another Kruskal–Wallis test was performed to detect statistical significance among these groups.

2.2. Spatial Data Analysis

For the spatial distribution analysis, we needed to correlate the GPS position of the drone with the sharks observed. The DJI MINI 2 records basic telemetry in the subtitles em-

bedded in the video files. Data such as camera settings, GPS coordinates (10 m resolution), distance from the pilot, height, and speed are recorded for each second of the video.

We used ffmpeg to extract subtitles from the videos, generating the corresponding SRT files. To aid in tracking sharks and correlating their observation times in the video with the SRT file records, we developed a hybrid Python/AppleScript application. The output of this application is a table for each video, where each row represents a shark observation and includes GPS and geometrical data.

Figure 2 illustrates the Python version 3.9.0/AppleScript version 2.8 application's interface. The application launches QuickTime Player, allowing the operator to navigate the video. When a shark is observed, the operator can use the mouse to draw a line on the shark. The application records the video time in seconds of the observation and other geometrical data. At the end of the process, a CSV file is generated for each video (Table 3), containing the following fields:

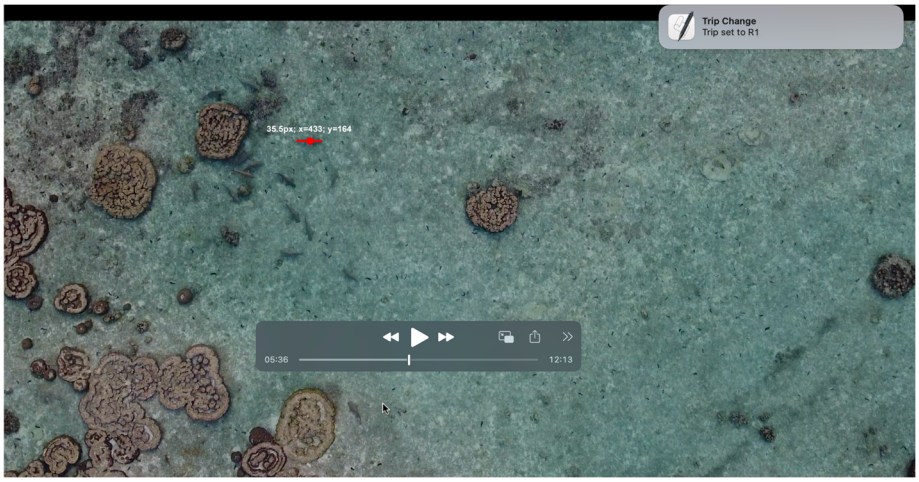


Figure 2. Python/AppleScript application's interface. The red line indicates the shark's length expressed in pixels.

- Leg of the transect (A1: first journey; R1: first return; A2: second journey; R2: second return);
- Video time in seconds of the observation;
- Position on the screen (x,y);
- Length of the line drawn on the individual in pixels;
- Sector, representing the actual transect sector, as explained below;
- GPS coordinates.

Table 3. Example of a CSV table produced by the Python/AppleScript application for a single video.

Transect Leg	Time	Screen_x	Screen_y	Length	Sector	Shark_Gps_Long	Shark_Gps_Lat
A1	120.6	653	72	33.9	6	99.8333	10.0646
A2	371.6	299	136	25.1	1	99.8312	10.0641
A2	476.4	382	28	13.9	7	99.8334	10.0646
A2	512	611	86	22.8	9	99.8342	10.0648
R2	526.2	426	678	20.7	9	99.8342	10.0648
R2	558.2	260	621	16.4	7	99.8337	10.0647

To conduct statistical tests, we divided the transect into 9 sectors, each measuring 40 m in length and approximately 41 m in width (corresponding to the camera footprint width calculated earlier). Figure 3 provides a georeferenced map created with QGIS, illustrating the layout of these sectors.

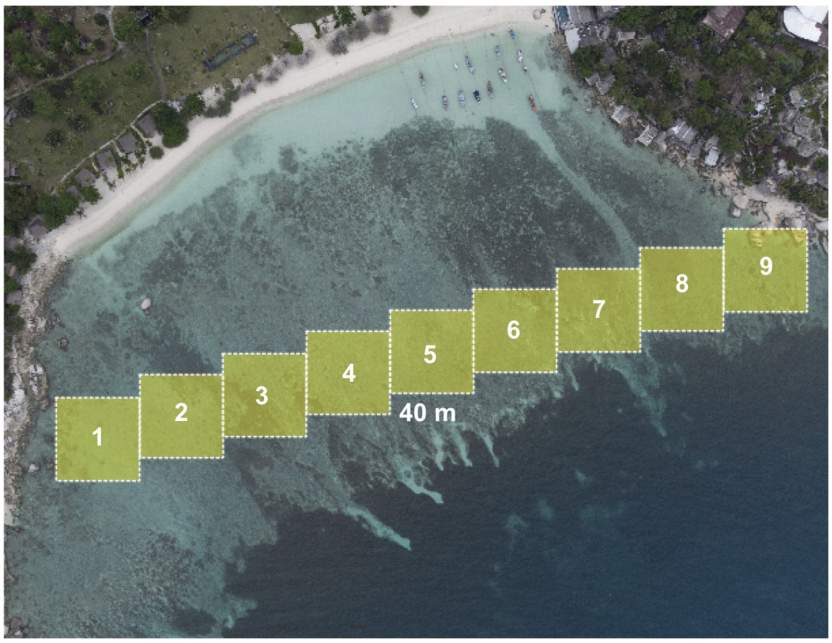


Figure 3. Map of the 9 sectors (40 m × 41 m) in which the transect was divided.

We used R to compile the tables generated by the Python/AppleScript application into three tables, each referred to as a 'sector-abundance table'. These tables document the number of observations within each sector for each respective time slot (Table 4). For the spatial distribution analysis, only one leg of the transect was used. Leg A1 was used for the morning, while the leg corresponding to nMax was used for the afternoon and evening.

Table 4. The 3 sector-abundance tables, one for each time slot, reporting the number of sharks observed and measured.

Sector Number	Sector Abundance 07:00	Sector Abundance 13:00	Sector Abundance 18:00
1	29	2	3
2	13	0	3
3	5	0	3
4	36	2	6
5	43	1	10
6	31	2	3
7	22	9	13
8	33	1	10
9	22	0	3

A Chi-squared test was conducted on each table to assess its distribution. The 3 Abundance-Sectors tables were compared using the Kruskal–Wallis test to assess the significance of the distribution among the 3 time slots.

2.3. Population Structure Analysis

The length of the lines drawn on the individuals using the developed Python/AppleScript application was used to categorize the population into two groups: juveniles and adults.

If we plot the length values of all the recorded sharks (Figure 4), we can observe that nearly 80% of the sharks' lengths fall within the range of 30 to 50 pixels. Between 30 and approximately 18 pixels, the curve steepens due to the scarcity of individuals within this range (less than 7%). Below 18 pixels, the curve gradually levels off.

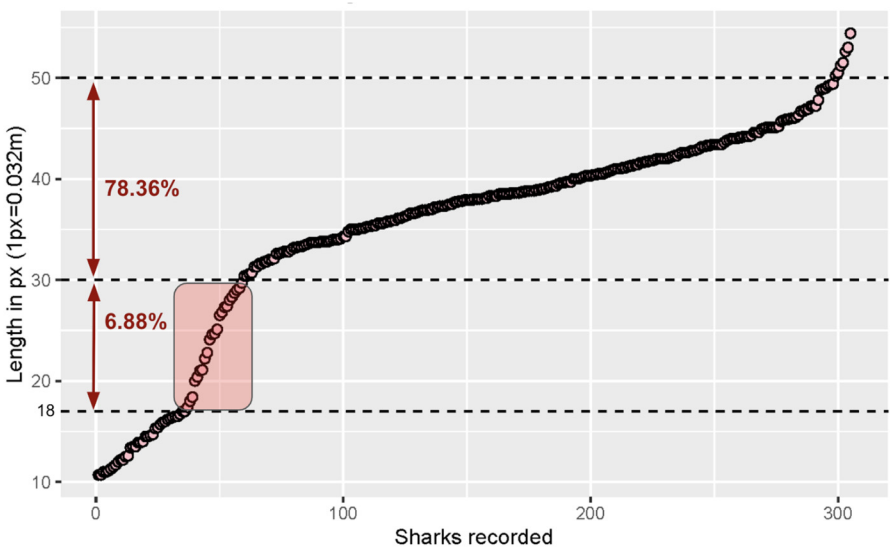


Figure 4. Length value of all the recorded sharks expressed in pixels.

Length values, measured from an aerial perspective, may be considered the PCL (Pre-Caudal Length) due to the limited visibility of the caudal fin when observed from 30 m above and under 0.5–1 m of water.

Measuring errors can potentially occur with this method due to subjectivity and image distortion. As a result, these length measurements on the screen primarily serve a comparative purpose and are influenced by the screen size on which the software is employed. For this study, we utilized a 13.3-inch screen with an effective resolution of 2560 × 1600. The actual resolution was scaled down by the Operating System to 1280 × 800. To determine the corresponding value in meters for 1 pixel, we calculated the Ground Sample Distance (GSD) based on the actual screen resolution. In our case, the obtained GSD value is as follows:

$$\text{GSD} = \frac{\text{SensorWidth} \times \text{Altitude}}{\text{FocalLength} \times \text{ImageWidth}} = \frac{6.17\ \text{mm} \times 30\ \text{m}}{4.49\ \text{mm} \times 1280\ \text{px}} = 0.032\ \text{m/px}$$

A single pixel on the screen, therefore, equals 0.032 m.

From the literature, we know that *C. melanopterus* reaches maturity starting from a Total Length of 93 cm [7].

We can calculate the corresponding PCL using a conversion formula for a morphologically similar species (*Carcharhinus brachyurus*) [31]:

$$\text{TL} = a + b * \text{PCL} = 10.270\ \text{cm} + 1.289 * \text{PCL}$$

where *a* and *b* are the conversion factors reported for *Carcharhinus brachyurus.*

Therefore, we have derived the following expression for the PCL:

$$\text{PCL} = \frac{\text{TL} - \text{a}}{\text{b}} = \frac{93\ \text{cm} - 10.270\ \text{cm}}{1.289} = 64.18\ \text{cm}$$

According to this, the minimal PCL for maturity is about 64.18 cm.

Then, we converted the obtained PCL back into pixels using the display's GSD and obtained a length of 20.06 pixels:

$$\text{LengthInPixels} = \frac{64.18\ \text{cm}}{\text{GSD}} = \frac{64.18\ \text{cm}}{3.2\ \text{cm/px}} = 20.06\ \text{px}$$

Therefore, individuals with a length less than 20 pixels were considered juveniles.

This hypothesis is corroborated by a boxplot of the measured lengths (Figure 5). The plot shows all the values below 20 pixels as outliers, where the length < Q1 − 1.5 × IQR.

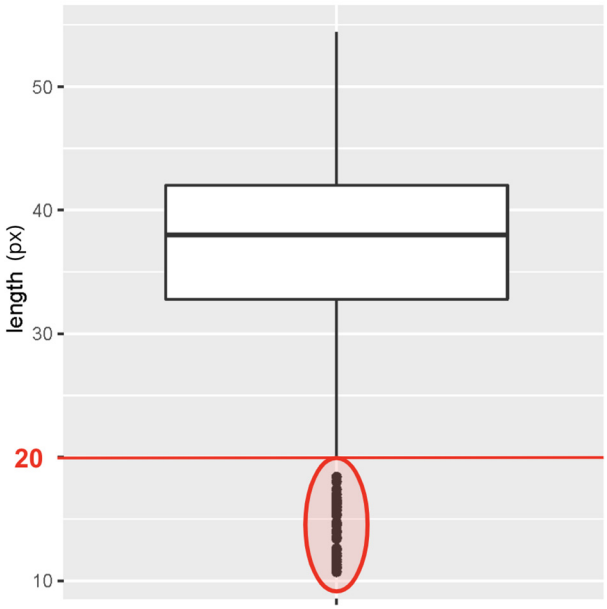


Figure 5. Boxplot of the measured lengths. Values below 20 px are considered outliers (red circle and line).

Once juveniles were separated from adults, we analyzed the abundance ratio of juveniles/adults among the 3 time slots. After that, we built 3 new sector-abundance tables only for juvenile individuals, and we performed a Kruskal–Wallis test on these 3 groups in order to identify sector preferences in juveniles.

2.4. Sex Ratio Surveys

From 2020 to 2022, we conducted an underwater video survey to determine the sex of the individuals (Table 5).

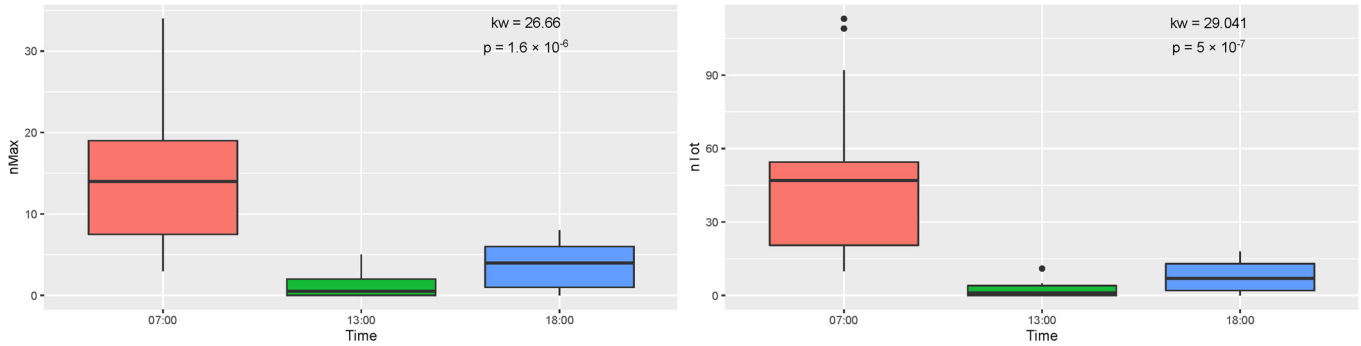
Table 5. Data from 2020–2022 underwater video surveys in order to determine the sex of the adult individuals.

Date	Time	Females	Males
07 March 2020	08:30	6	0
08 March 2020	09:00	2	0
08 March 2020	18:00	1	0
17 September 2020	09:00	1	0
05 July 2021	09:00	5	0
06 July 2021	10:00	3	0
21 September 2021	10:00	2	0
21 September 2022	09:00	1	0
23 September 2022	07:30	0	0
24 September 2022	07:00	4	0
26 September 2022	08:30	5	0
28 September 2022	08:00	5	0
Total		35	0

3. Results

3.1. Abundance and Activity in Relation to the Time Slots

The Kruskal–Wallis test performed on the abundance values (nMax) grouped by the three time slots evidenced a highly statistically significant relationship between time and abundance (kw = 26.66; $p < 0.001$) (Figure 6a). The abundance is higher at 07:00 am. Similarly, we grouped activity values (nTot) by the three time slots (07:00, 13:00, 18:00), creating three groups. We performed a Kruskal–Wallis test on these groups. The result evidenced a high statistically significant relationship between time and activity (kw = 29.04; $p < 0.001$) (Figure 6b). The activity is higher at 07:00 am.



(**a**) (**b**)

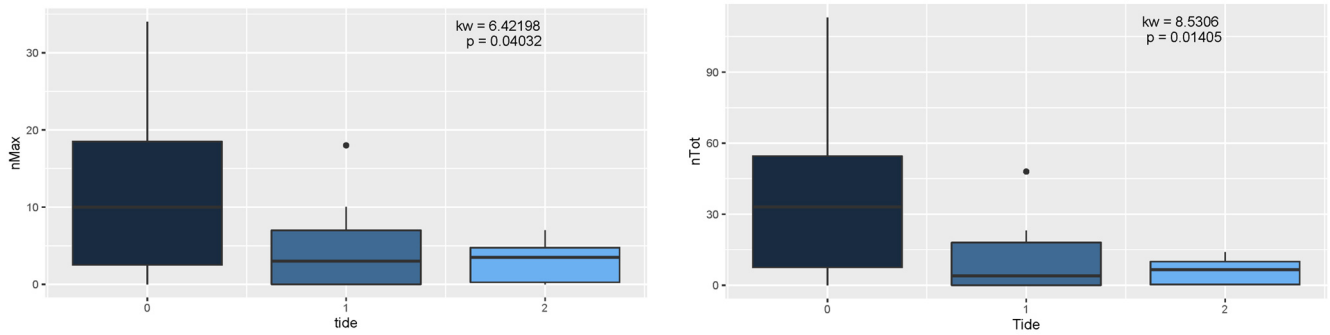
Figure 6. Abundance and activity of the sharks during daytime: (**a**) time vs. abundance; (**b**) time vs. activity.

3.2. Abundance and Activity in Relation to the Environmental Factors

In this section, we present the results obtained performing the Kruskal–Wallis test on the groups formed by aggregating abundance (nMax) and activity (nTot) by the classes of values that describe each environmental factor.

3.2.1. Tide

We found a statistically significant relationship (kw = 6.42; $p = 0.04$) between the tide height and the abundance (nMax). In particular, sharks appear to be more abundant during low tide conditions (Figure 7a).



(**a**) (**b**)

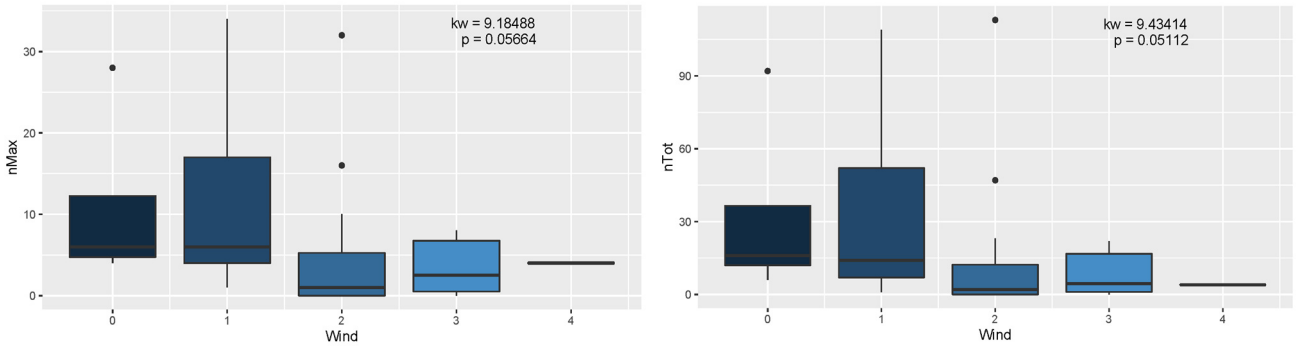
Figure 7. Abundance and activity of the sharks according to tides: (**a**) tide vs. abundance; (**b**) tide vs. activity. Legend: 0 = low tide; 1 = medium tide; 2 = high tide.

Also, activity (nTot) shows a statistically significant relationship with the tide (kw = 8.53; $p = 0.014$) (Figure 7b). In particular, sharks are more active during low tide conditions.

3.2.2. Wind

A nearly significant relationship is observed (kw = 9.18; $p = 0.057$) between abundance (nMax) and wind: abundance is higher under lower wind conditions (0 and 1) (Figure 8a).

Similar results were found for interceptability (nTot), which is significantly associated with low wind conditions (0 and 1) (Figure 8b).

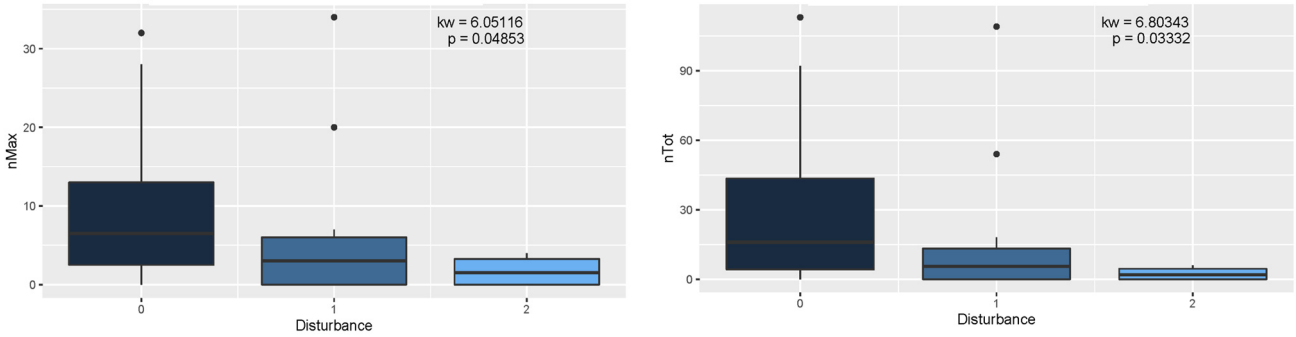


(**a**) (**b**)

Figure 8. Abundance and activity of the sharks according to wind conditions: (**a**) wind vs. abundance; (**b**) wind vs. activity. Legend: 0: absent (0 m/s wind speed); 1: weak (1–2 m/s wind speed); 2: medium (3–5 m/s wind speed); 3: strong (5–10 m/s wind speed); 4: very strong (>10 m/s wind speed).

3.2.3. Anthropogenic Disturbance

Abundance (nMax) is significantly correlated with anthropogenic disturbance (kw = 6.05; $p = 0.048$) (Figure 9a), as is activity (nTot) (kw = 6.8; $p = 0.033$) (Figure 9b). Sharks are more abundant and active under lower levels of anthropogenic disturbance.

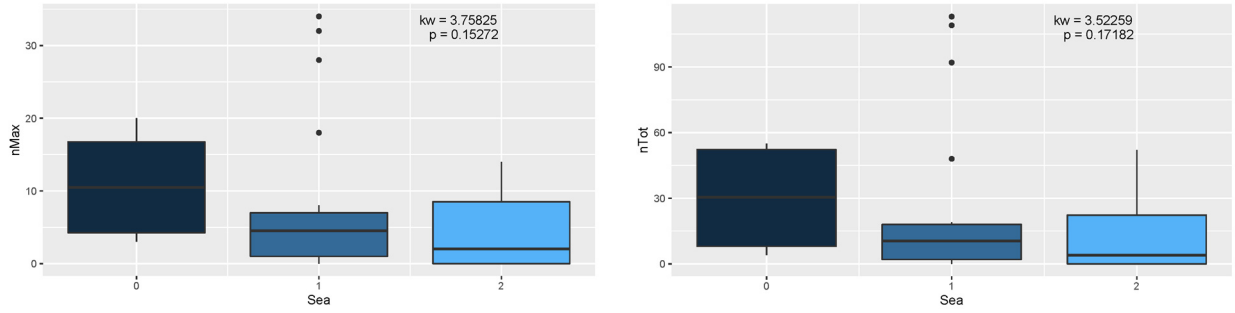


(**a**) (**b**)

Figure 9. Abundance and activity of the sharks and anthropogenic disturbance: (**a**) anthropogenic disturbance vs. abundance; (**b**) anthropogenic disturbance vs. activity. Legend: 0: absent; 1: snorkeling/kayaking; 2: motorboat.

3.2.4. Sea Condition

Throughout the observed period, wave motion within the bay remained consistently low, with occasional mild fluctuations. The graphical analysis suggests a potential correlation between the absence of substantial wave motion and both abundance (Figure 10a) and activity (Figure 10b). Nevertheless, it is important to note that these relationships did not attain statistical significance.

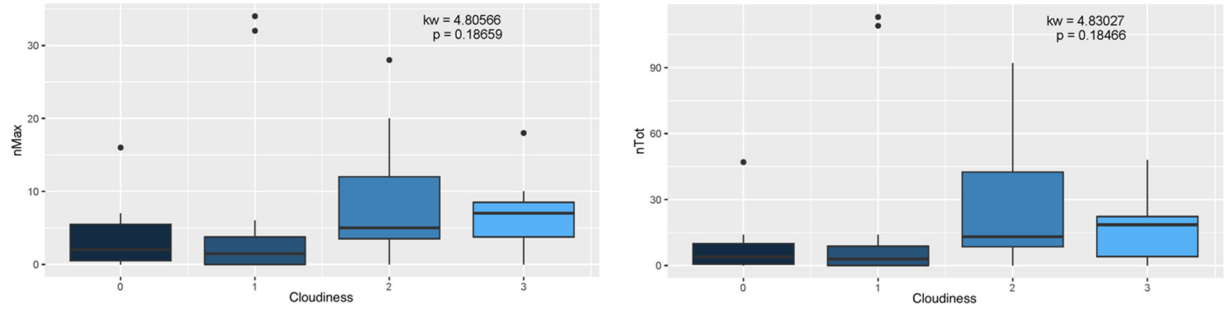


(**a**) (**b**)

Figure 10. Abundance and activity of the sharks and sea conditions: (**a**) sea condition vs. abundance; (**b**) sea condition vs. activity. Legend: 0 (0–1 Beaufort scale): flat; 1: quiet (2–3 Beaufort scale); 2: almost quiet (4 Beaufort scale).

3.2.5. Cloudiness

For both abundance (nMax) and activity (nTot), the graphs exhibit a discernible association with cloud cover, with higher values of abundance and interceptability occurring under cloudy conditions. Nevertheless, it is important to emphasize that these associations do not achieve statistical significance (abundance in Figure 11a; activity in Figure 11b).



(**a**) (**b**)

Figure 11. Abundance and activity of the sharks and cloudiness: (**a**) cloudiness vs. abundance; (**b**) cloudiness vs. activity. Legend: 0: clear (0–2 Oktas); 1: partly cloudy (3–5 Oktas); 2: cloudy (6–8 Oktas); 3: rain (after/before).

3.3. Spatial Distribution

The chi-square test performed on the three sector-abundance tables (Table 4) revealed that for all three time slots, the distribution of individuals among the nine sectors significantly deviates from a normal distribution. Specifically, we obtained the following:

- Abundance-sector table at 07:00, $p < 0.001$;
- Abundance-sector table at 13:00, $p < 0.001$;
- Abundance-sector table at 18:00, $p = 0.007$.

The graphical representation of the three tables can be seen, respectively, in Figure 12a–c. The Kruskal–Wallis test across the three sector-abundance tables yielded kw = 19.91 and $p < 0.001$, indicating statistical significance in the relationship between time slot and spatial distribution. A composite graph depicting the spatial distribution across the three time slots can be seen in Figure 12d.

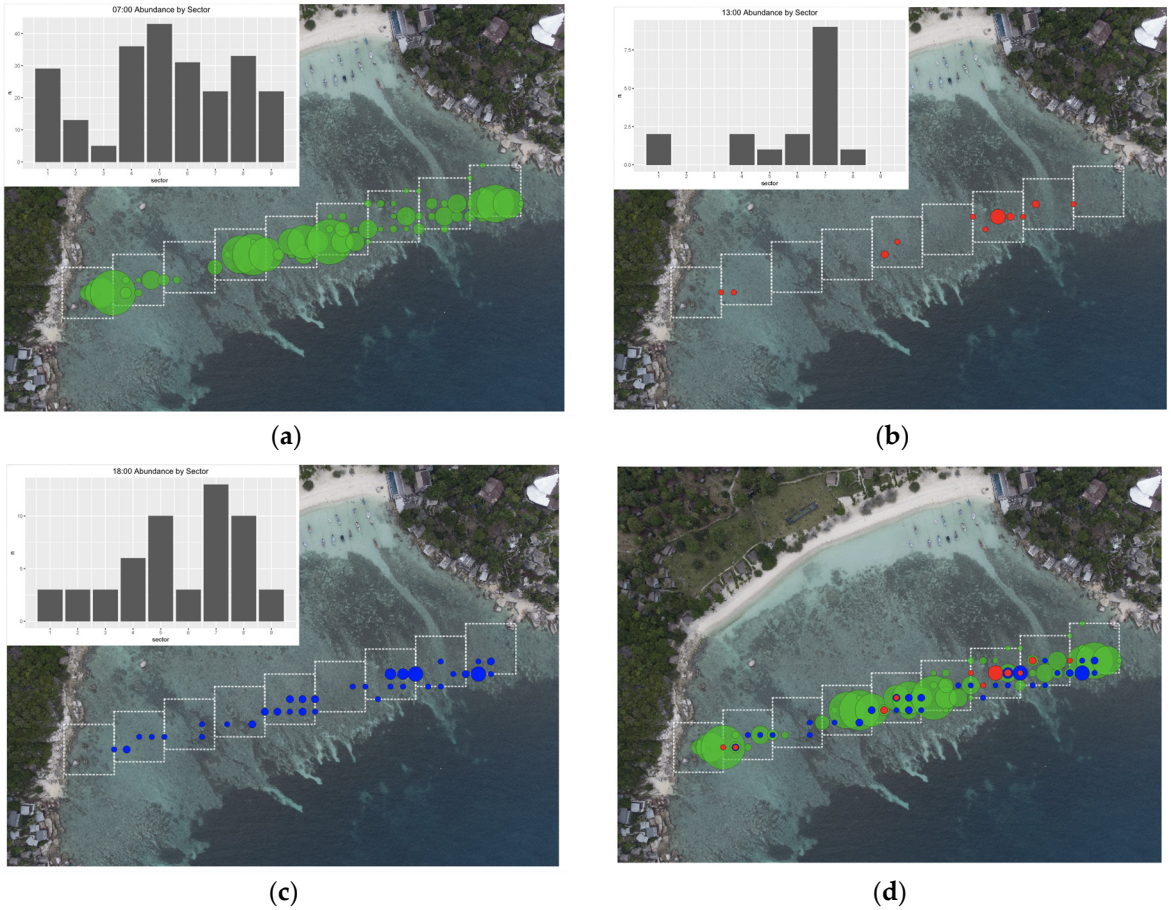


Figure 12. Abundance of the sharks during daytime in the different sectors. (**a**) Abundance by sector at 07:00; (**b**) abundance by sector at 13:00; (**c**) abundance by sector at 18:00; (**d**) composite representation of the abundance by sector: 07:00 (green), 13:00 (red), 18:00 (blue). White dotted represent the 9 sectors (40 m × 41 m) in which the transect was divided.

3.4. Population Structure and Spatio-Temporal Distribution of Juveniles

Once we have separated the juveniles from the adults, we can plot their abundance ratio across different time slots (Figure 13). In the morning, only 3.4% of the recorded individuals were juveniles. In the afternoon, almost all individuals were juveniles. In the evening, about 28% of the individuals were juveniles.

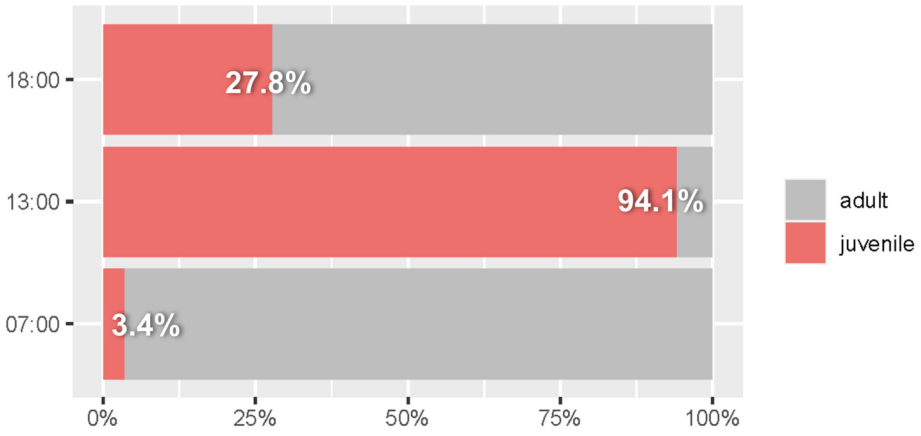


Figure 13. Juveniles/adults abundance ratio within the 3 time slots (juveniles in red).

Regarding the spatial distribution of juveniles, when conducting the Kruskal–Wallis test for the three time slots and their respective tables (abundance, juveniles, sectors), it is evident that there is no significant relationship between the occupied sectors and time slot for juveniles (kw = 1.77; $p = 0.410$). In fact, they are distributed similarly across all three time slots, with a significant preference for sector number 7 ($p < 0.001$), as can be seen in Figure 14.

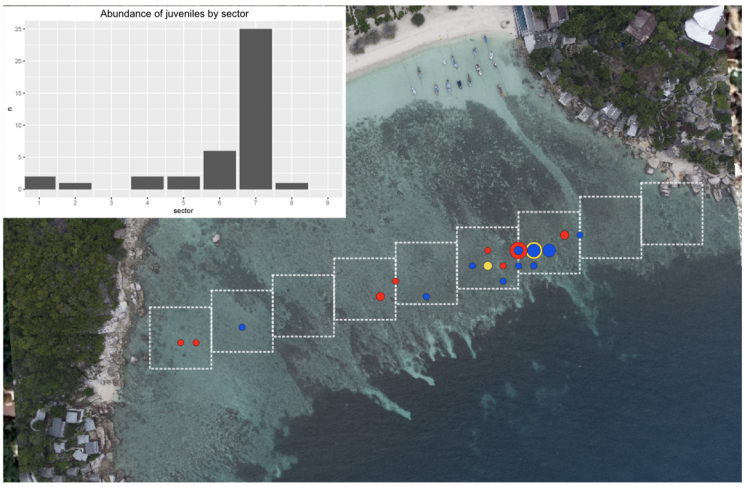


Figure 14. Composite graph depicting the distribution of juveniles across the three time slots. Legend: 07:00 (yellow), 13:00 (red), 18:00 (blue); white dotted represent the 9 sectors (40 m × 41 m) in which the transect was divided.

3.5. Sex Ratio

From 2020 to 2022, we conducted an underwater video survey to determine the sex of the individuals. Among the 35 adult individuals recorded, no male sharks were recorded; only females were present in the bay (Figure 15).

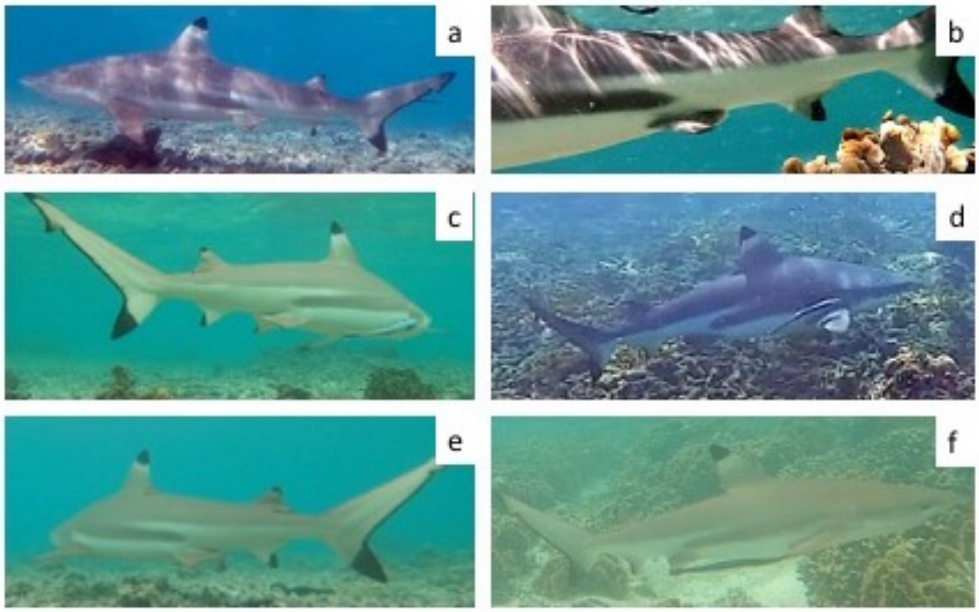


Figure 15. Some of the adult individuals observed underwater between 2020 and 2022. All observed individuals were females. (**a**) Specimen observed on 05 July 2021; (**b**) specimen observed on 17/09/2020; (**c**) specimen observed on 23 September 2022; (**d**) specimen observed on 06 July 2021; (**e**) specimen observed on 24 September 2022; (**f**) specimen observed on 17 September 2020.

4. Discussion

We proposed a method to study the spatio-temporal distribution and population structure of *Carcharhinus melanopterus* using UAVs in shallow waters. Although the study's short duration limits the conclusiveness of our results, they are still relevant to the specific time period during which the research was conducted. The proposed method demonstrates the potential of using an entry-level UAV with a minimal budget to collect and analyze data in a semi-automatic way, using the support of a desktop application to count, track, and measure the individuals for further population structure analyses.

UAV surveys provide the advantage of studying aquatic animals without causing interaction or disturbance, provided that basic requirements are met [24]. However, this approach is limited by factors such as local regulations, battery life, the effort required from UAV operators, and, eventually, extensive video analyses. In this study, a fully charged battery allowed for two round trips across a 360 m transect at a speed of 2 m/s, resulting in 12 min of video recording for each of the three time slots. Finer time scales can be achieved with multiple batteries and/or a charger, but the storage and effort for video analysis must also be considered.

Although automated flight is widely available on consumer drones or through third-party mobile apps, it is not allowed in countries such as Thailand, so it was not taken into consideration.

Recorded adult sharks could be easily spotted in the videos by human operators under all conditions encountered during the study, due to their continuous movements and thanks to shallow water. However, manual data extraction from videos becomes impractical with extensive recordings. While ML/AI techniques have proven useful for detecting sharks under specific conditions [25,26], they were challenging to implement in this study due to the varied substrate (rocks, corals, sand), superficial water movements, and variable light. Moreover, due to the presence of swimmers and boats, we had to maintain a height of 30 m according to local regulations. This resulted in a strip transect 40 m wide that, considering the length of the animals to detect, would be computationally demanding to analyze using Object Tracking. Due to the wide transect strip, juveniles were harder to spot and probably impossible to detect using ML/AI.

Considering a UAV flying a transect and the continuous shark motion, algorithms like Optical Flow could initially detect pixel groups that deviate from the UAV's linear motion, allowing the application of Object Detection only to specific image regions. Combining these techniques, Object Tracking can be theoretically achieved, preventing double counting and providing insights into the motion trajectory and speed of the animals.

The correlation between high abundance/activity and low anthropogenic disturbance suggests that human activities may exert some pressure on this species.

We found high abundance/activity correlated with low tides and time of day, with a high preference for morning time. In 9 h and 52 min of total video recordings, no bursts, sudden movements, or feeding behaviors were recorded. All individuals roamed at a constant speed all the time. This may suggest the bay is not a feeding area for adults, at least during day time. Thermoregulatory behavior in shallow bays to enhance embryo development has been extensively reported for coastal shark species [27]. In our case, this hypothesis is corroborated by the underwater survey that resulted in only females being observed.

Some sectors presented more abundance/activity than others; this may be due to local temperature, anthropic disturbance, or other parameters not recorded in this study.

Juveniles' spatio-temporal analysis revealed that they constituted a consistent percentage of the individuals at 18:00 and 13:00 due to the low presence of adults in these time slots. *Carcharhinus melanopterus* juveniles are characterized by limited motion [28]; they remain around nursery areas at all times, while adults tend to leave the bay when conditions change. Their distribution was similar across all three time slots, with a significant preference for sector number 7, for which we do not have enough data to speculate about.

Nursery areas for coastal sharks have been defined by three primary criteria for newborn or young-of-the-year individuals [29]: (1) density in the area is greater than the mean density over all areas; (2) site fidelity is greater than the mean site fidelity for all areas; (3) the area is repeatedly used across years, whereas others are not.

Tien Og is named Shark Bay due to the abundance of sharks throughout the year. However, since we cannot provide a comparison with adjacent areas, we cannot define Tien Og bay as a nursery area. Considering the low mobility of *Carcharhinus melanopterus* juveniles, their constant presence in the bay paired, and the presence of only adult females, we can hypothesize that the area is involved in the reproduction of *Carcharhinus melonapterus*, although the contribution to the adult stock remains unknown. *Carcharhinus melanopterus* may visit the bay during specific times of the day to raise body temperature, potentially facilitating an increase in metabolic rate and/or gestation, and abandon it during the midday hours when temperatures rise excessively. During this study, around 14:00, the water temperature in the bay, as recorded by an Olympus TG-5 camera, reached 31.5 °C.

5. Conclusions

The study encompassed a population of *Carcharhinus melanopterus* in Tien Og Bay on Koh Tao Island, Thailand. Aerial surveys were conducted using a UAV to study the spatio-temporal distribution, abundance, and groups composition of the species. The proposed method has proven to be inexpensive, noninvasive, effective overall, and capable of providing, even in rather short time intervals, valuable information on the ecology of a species that is not always easy to study. In particular, the use of UAVs has allowed us to collect data on several different individuals within defined transects and considering different environmental variables. Further data collection campaigns could be useful to improve the method and the use of UAVs; however, this preliminary study demonstrates how the use of this technology can represent valid support to researchers for the collection of data on the spatial ecology of coastal sharks in shallow waters.

Author Contributions: Conceptualization, A.D.T., G.G. and E.S.; methodology, A.D.T., G.G. and E.S.; software, A.D.T., validation, F.L.L., E.S. and G.G., formal analysis, A.D.T., investigation, A.D.T. and S.S.; resources, A.D.T. and S.S.; data curation, A.D.T.; writing—original draft preparation, A.D.T., E.S. and G.G.; writing—review and editing, F.L.L., E.S. and G.G.; supervision, E.S. and G.G. All authors have read and agreed to the published version of the manuscript.

Funding: This research received no external funding.

Data Availability Statement: Data is contained within the article.

Acknowledgments: The drone, purchased in Thailand, was registered—together with the operator—with the Civil Aviation Authority of Thailand (CAAT) and the National Broadcasting and Telecommunications Commission (NBTC). Insurance was also stipulated to cover accidents up to 1 million baht, as required by law.

Conflicts of Interest: The authors declare no conflict of interest.

References

1. Hobson, E.S. Feeding Behavior in Three Species of Sharks. *Pac. Sci.* **1963**, *17*, 171–194.
2. Stevens, J.D. Life-History and Ecology of Sharks at Aldabra Atoll, Indian Ocean. *Proc. R. Soc. Lond. B.* **1984**, *222*, 79–106. [CrossRef]
3. Sandin, S.A.; Smith, J.E.; DeMartini, E.E.; Dinsdale, E.A.; Donner, S.D.; Friedlander, A.M.; Konotchick, T.; Malay, M.; Maragos, J.E.; Obura, D.; et al. Baselines and Degradation of Coral Reefs in the Northern Line Islands. *PLoS ONE* **2008**, *3*, e1548. [CrossRef]
4. Cortes, E. Standardized Diet Compositions and Trophic Levels of Sharks. *ICES J. Mar. Sci.* **1999**, *56*, 707–717. [CrossRef]
5. Last, P.R.; Stevens, J.D. *Sharks and Rays of Australia*; Harvard University Press: Cambridge, MA, USA, 2009; ISBN 978-0-674-03411-2.
6. Chin, A.; Simpfendorfer, C.; Tobin, A.; Heupel, M. Validated Age, Growth and Reproductive Biology of Carcharhinus Melanopterus, a Widely Distributed and Exploited Reef Shark. *Mar. Freshw. Res.* **2013**, *64*, 965. [CrossRef]
7. Lyle, J. Observations on the Biology of *Carcharhinus cautus* (Whitley), *C. melanopterus* (Quoy & Gaimard) and *C. fitzroyensis* (Whitley) from Northern Australia. *Mar. Freshw. Res.* **1987**, *38*, 701. [CrossRef]

8. White, W.T. *Economically Important Sharks & Rays of Indonesia = Hiu dan Pari Yang Bernilai Ekonomis Penting di Indonesia*; Australian Centre for International Agricultural Research: Canberra, Australia, 2006; ISBN 978-1-86320-517-7.
9. Chin, A.; Tobin, A.; Simpfendorfer, C.; Heupel, M. Reef Sharks and Inshore Habitats: Patterns of Occurrence and Implications for Vulnerability. *Mar. Ecol. Prog. Ser.* **2012**, *460*, 115–125. [CrossRef]
10. Mukharror, D.A.; Susiloningtyas, D.; Handayani, T.; Pridina, N. Blacktip Reefshark (Carcharhinus Melanopterus) Individual's Identification in Morotai Waters Using Its Fin's Natural Markings. *AIP Conf. Proc.* **2019**, *2202*, 020085.
11. Lyle, J.M.; Timms, G.J. Predation on Aquatic Snakes by Sharks from Northern Australia. *Copeia* **1987**, *1987*, 802. [CrossRef]
12. Papastamatiou, Y.P.; Lowe, C.G.; Caselle, J.E.; Friedlander, A.M. Scale-dependent Effects of Habitat on Movements and Path Structure of Reef Sharks at a Predator-dominated Atoll. *Ecology* **2009**, *90*, 996–1008. [CrossRef]
13. Mourier, J.; Vercelloni, J.; Planes, S. Evidence of Social Communities in a Spatially Structured Network of a Free-Ranging Shark Species. *Anim. Behav.* **2012**, *83*, 389–401. [CrossRef]
14. Klimley, A.P.; Le Boeuf, B.J.; Cantara, K.M.; Richert, J.E.; Davis, S.F.; Van Sommeran, S.; Kelly, J.T. The Hunting Strategy of White Sharks (Carcharodon Carcharias) near a Seal Colony. *Mar. Biol.* **2001**, *138*, 617–636. [CrossRef]
15. Myrberg, A.A., Jr. Distinctive Markings of Sharks: Ethological Considerations of Visual Function. *J. Exp. Zool.* **1990**, *256*, 156–166. [CrossRef]
16. Butcher, P.A.; Colefax, A.P.; Gorkin, R.A.; Kajiura, S.M.; López, N.A.; Mourier, J.; Purcell, C.R.; Skomal, G.B.; Tucker, J.P.; Walsh, A.J.; et al. The Drone Revolution of Shark Science: A Review. *Drones* **2021**, *5*, 8. [CrossRef]
17. Leonetti, F.L.; Bottaro, M.; Giglio, G.; Sperone, E. Studying Chondrichthyans Using Baited Remote Underwater Video Systems: A Review. *Animals* **2024**, *14*, 1875. [CrossRef] [PubMed]
18. Colefax, A.; Kelaher, B.; Pagendam, D.E.; Butcher, P. Assessing White Shark (Carcharodon Carcharias) Behavior Along Coastal Beaches for Conservation-Focused Shark Mitigation. *Front. Mar. Sci.* **2020**, *7*, 265. [CrossRef]
19. Raoult, V.; Broadhurst, M.; Peddemors, V.; Williamson, J.; Gaston, T. Resource Use of Great Hammerhead Sharks (Sphyrna Mokarran) off Eastern Australia. *J. Fish Biol.* **2019**, *95*, 1430–1440. [CrossRef]
20. Gore, M.; Abels, L.; Wasik, S.; Saddler, L.; Ormond, R. Are Close-Following and Breaching Behaviours by Basking Sharks at Aggregation Sites Related to Courtship? *J. Mar. Biol. Assoc. UK* **2018**, *99*, 693. [CrossRef]
21. Dines, S.; Gennari, E. First Observations of White Sharks (Carcharodon Carcharias) Attacking a Live Humpback Whale (Megaptera Novaeangliae). *Mar. Freshw. Res.* **2020**, *71*, 1205–1210. [CrossRef]
22. Doan, M.; Kajiura, S. Adult Blacktip Sharks (Carcharhinus Limbatus) Use Shallow Water as a Refuge from Great Hammerheads (Sphyrna Mokarran). *J. Fish Biol.* **2020**, *96*, 1530–1533. [CrossRef] [PubMed]
23. Kiszka, J.; Mourier, J.; Gastrich, K.; Heithaus, M. Using Unmanned Aerial Vehicles (UAVs) to Investigate Shark and Ray Densities in a Shallow Coral Lagoon. *Mar. Ecol. Prog. Ser.* **2016**, *560*, 237–242. [CrossRef]
24. Bennett, M.K.; Younes, N.; Joyce, K. Automating Drone Image Processing to Map Coral Reef Substrates Using Google Earth Engine. *Drones* **2020**, *4*, 50. [CrossRef]
25. Yeemin, T.; Sutthacheep, M.; Pettongma, R. Coral Reef Restoration Projects in Thailand. *Ocean Coast. Manag.* **2006**, *49*, 562–575. [CrossRef]
26. Scott, C.M.; Mehrotra, R.; Hein, M.Y.; Moerland, M.S.; Hoeksema, B.W. Population Dynamics of Corallivores (Drupella and Acanthaster) on Coral Reefs of Koh Tao, a Diving Destination in the Gulf of Thailand. *Raffles Bull. Zool.* **2017**, *65*, 68–79.
27. Wongthong, P.; Harvey, N. Integrated Coastal Management and Sustainable Tourism: A Case Study of the Reef-Based SCUBA Dive Industry from Thailand. *Ocean Coast. Manag.* **2014**, *95*, 138–146. [CrossRef]
28. Weterings, R. A GIS-Based Assessment of Threats to the Natural Environment on Koh Tao, Thailand. *Kasetsart J. (Nat. Sci.)* **2011**, *45*, 743–755.
29. Hein, M.Y.; Lamb, J.B.; Scott, C.; Willis, B.L. Assessing Baseline Levels of Coral Health in a Newly Established Marine Protected Area in a Global Scuba Diving Hotspot. *Mar. Environ. Res.* **2015**, *103*, 56–65. [CrossRef]
30. Scaps, P.; Scott, C. An Update to the List of Coral Reef Fishes from Koh Tao, Gulf of Thailand. *Check List* **2014**, *10*, 1123–1133. [CrossRef]
31. Mas, F.; Forselledo, R.; Domingo, A. Length-length relationships for six pelagic shark species commonly caught in the southwestern Atlantic Ocean. *Collect. Vol. Sci. Pap. ICCAT* **2014**, *70*, 2441–2445.

Disclaimer/Publisher's Note: The statements, opinions and data contained in all publications are solely those of the individual author(s) and contributor(s) and not of MDPI and/or the editor(s). MDPI and/or the editor(s) disclaim responsibility for any injury to people or property resulting from any ideas, methods, instructions or products referred to in the content.